

Efficient 1,4-Addition of Enones and Boronic Acids Catalyzed by a Ni–Zn Hydroxyl Double Salt-Intercalated Anionic Rhodium(III) Complex

Takayoshi Hara,[†] Nozomi Fujita,[†] Nobuyuki Ichikuni,[†] Karen Wilson,[‡] Adam F. Lee,[‡] and Shogo Shimazu^{*†}

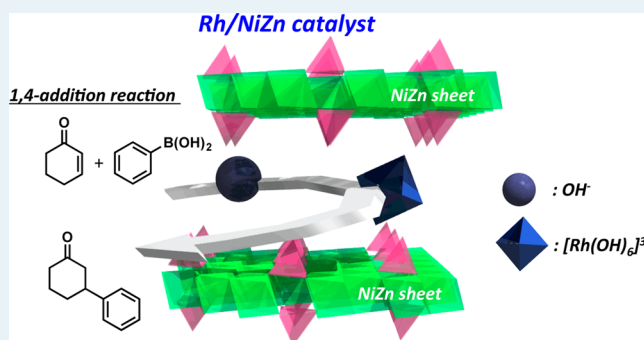
[†]Department of Applied Chemistry and Biotechnology, Graduate School of Engineering, Chiba University, 1-33, Yayoi, Inage, Chiba 263-8522, Chiba, Japan

[‡]European Bioenergy Research Institute, School of Engineering and Applied Sciences, Aston University, Aston Triangle, Birmingham B4 7ET, U.K.

S Supporting Information

ABSTRACT: Intercalation of an in situ prepared $[\text{Rh}(\text{OH})_6]^{3-}$ complex into an anion exchangeable Ni–Zn layered hydroxy double salt (Rh/NiZn) was demonstrated. The resulting Rh/NiZn effectively catalyzed the 1,4-addition of diverse enones and phenylboronic acids to their corresponding β -substituted carbonyl compounds. In the case of 2-cyclohexen-1-one and phenylboronic acid, a turnover frequency (TOF) of 920 h^{-1} based on Rh was achieved. The $[\text{Rh}(\text{OH})_6]^{3-}$ complex maintained its original monomeric trivalent state within the NiZn interlayer following catalysis, attributable to a strong electrostatic interaction between the NiZn host and anionic Rh(III) complex.

KEYWORDS: Ni–Zn hydroxyl double salt, anion exchange, intercalation, rhodium, 1,4-addition



1. INTRODUCTION

Although anion-exchangeable clays are relatively rare compared with cationic clays in nature, their high surface area, sorptive, and ion-exchange properties have been utilized in catalytic applications for decades.¹ Among these materials, layered hydroxy double salts (HDSs),² which consist of positively charged layers and exchangeable interlayer anions, have received considerable interest as anion-exchangeable layered compounds because of their potential applications as catalyst supports. The general formula of HDS families can be represented as $\text{M}^{2+}_{1-x}\text{M}^{2+}_{2x}(\text{OH})_2\text{A}^{n-}_{2x/n}\cdot m\text{H}_2\text{O}$ ($0.15 < x < 0.25$), where M^{2+} and M^{2+} are divalent metal cations such as Zn^{2+} , Cu^{2+} , Co^{2+} , or Ni^{2+} and A^{n-} represents various anions. We have continued to develop “intercalation catalysts” using a Ni–Zn mixed basic salt (NiZn), which is considered an HDS.³ By exploiting the anion-exchange ability of NiZn, researchers have investigated the intercalation of various guest anions, including simple inorganic anions⁴ such as AcO^- , NO_3^- , SO_4^{2-} , CO_3^{2-} , PO_4^{3-} , Cl^- , or Br^- ; anionic metal complexes;⁵ organic carboxylates;⁶ and sulfates or sulfonates⁷ into the NiZn interlayer. Our choice of NiZn as a catalyst support is motivated by the following advantages: (i) simple preparation, (ii) high crystallinity, (iii) isolation of anion-exchangeable sites and neighboring Zn^{2+} cations, and (iv) strong electrostatic interactions between the guest interlayer anions and the Zn^{2+} cations. We have recently demonstrated that a function-

integrated $[(\text{D-valine})\text{Pd}(\text{OH})_2]^-/\text{PO}_4^{3-}/\text{NiZn}$ intercalation catalyst effectively drives the aerobic oxidation of alcohols into their corresponding carbonyl compounds.^{3a} In this case, a Brønsted-basic PO_4^{3-} anion, intercalated into the NiZn interlayer along with the anionic Pd(II)-amino acid complex, was able to act as “a substrate activator”. Our recent success with the intercalation of well-defined anionic Pd(II)-hydroxide complexes prompted us to examine whether this general synthetic methodology could be extended to rhodium.

β -Substituted carbonyl compounds are versatile intermediates in the synthesis of high-value organic chemicals.⁸ Much attention has been devoted to the rhodium-catalyzed 1,4-addition reaction between arylboronic acids to form α,β -unsaturated carbonyl compounds since the first report by Miyaura et al. in 1997.⁹ Thereafter, the development of homogeneous chiral rhodium catalysts with various well-defined ligands was reported.¹⁰ However, to facilitate recycling of the expensive rhodium, numerous families of heterogeneous rhodium catalysts, including polymer-bound catalysts,¹¹ surface-immobilized catalysts,¹² and polymer-intercalated bimetallic nanoparticle catalysts¹³ have also been developed. Miyaura¹⁴ and Hayashi¹⁵ et al. reported that monovalent Rh hydroxide

Received: August 26, 2014

Revised: October 2, 2014

Published: October 6, 2014

species exhibited high catalytic activity toward the 1,4-addition reaction because the transmetalation of an aryl group from boron to rhodium occurs immediately. Here, we present a new strategy for the design of a novel immobilized Rh hydroxide complex catalyst based on the anion-exchange ability of NiZn and demonstrate the aforementioned 1,4-addition reaction by use of the resulting synthesized heterogeneous catalyst. In our catalyst system, monomeric trivalent Rh hydroxide $[\text{Rh}(\text{OH})_6]^{3-}$ acts as the catalytically active site, fixed within NiZn interlayers. Furthermore, the hydroxyl anion, which may activate phenylboronic acid, can also be integrated into the NiZn matrix together with the anionic Rh species. Because of the strong electrostatic interaction between the interlayer guest anion and the NiZn host, conventionally unstable monomeric $[\text{Rh}(\text{OH})_6]^{3-}$ species can be stabilized within the NiZn interlayer.

2. EXPERIMENTAL SECTION

2.1. Preparation of $\text{CH}_3\text{COO}^-/\text{NiZn}$. Acetate anion-intercalated Ni–Zn hydroxy double salt ($\text{CH}_3\text{COO}^-/\text{NiZn}$) was prepared according to the literature procedures.¹⁶ Ni(OCOCH_3)₂·4H₂O (134 mmol) and Zn(OCOCH_3)₂·2H₂O (66 mmol) were dissolved in deionized water (200 mL). The solution was hydrolyzed by heating in a Teflon-linked pressure bottle at 200 °C for 24 h. The resulting precipitates were filtered, washed with deionized water, and dried under vacuum, yielding ca. 5 g of Ni_{0.63}Zn_{0.37}(OCOCH_3)_{0.37}(OH)₂·1.93H₂O ($\text{CH}_3\text{COO}^-/\text{NiZn}$) as a light green powder.

2.2. Preparation of the Rh/NiZn Catalyst. The NiZn-intercalated $[\text{Rh}(\text{OH})_6]^{3-}$ complex (Rh/NiZn catalyst) was prepared by a simple intercalation technique. Na₃RhCl₆·nH₂O (Rh: 0.05 mmol, concentration of rhodium species was determined by AAS) was placed in a round-bottom flask, and the total volume was adjusted to 40 mL with deionized water. The red solution was heated with stirring at 50 °C for 30 min after addition of 10 M NaOH aq. (10 mL), turning the solution yellow. $\text{CH}_3\text{COO}^-/\text{NiZn}$ (1 g) was added to the resulting solution and stirred at 50 °C for 8 h. The obtained slurry was filtered, washed with deionized water, and dried under vacuum, yielding Rh/NiZn as a light green powder.

2.3. Typical Procedure for 1,4-Addition between 2-Cyclohexen-1-one and Phenylboronic Acid. Into a Schlenk tube with a reflux condenser, Rh/NiZn catalyst (0.034 g, Rh: 0.1 mol %), 2-cyclohexen-1-one (1 mmol), phenylboronic acid (1 mmol), 1,5-cyclooctadiene (6 μmol), toluene (2.5 mL), and H₂O (2.5 mL) were placed. The resulting mixture was heated at 100 °C for 1 h. After the reaction, biphenyl was added to the resulting mixture as an internal standard. The conversion and product yield were determined by GC analysis using an internal standard technique. After the removal of the Rh/NiZn catalyst by simple filtration, evaporation of the solvent followed by silica gel chromatography (*n*-hexane/ethyl acetate = 9/1) gave analytically pure 3-phenylcyclohexanone.

3. RESULTS AND DISCUSSION

Preparation of the rhodium hydroxy anion, $[\text{Rh}(\text{OH})_6]^{3-}$, via the hydrolysis of Rh(III) salts in alkaline water has been previously reported.¹⁷ In this work, the prepared Na₃RhCl₆·12H₂O¹⁸ was treated with an aqueous solution of 10 M NaOH. The coordinated structure of the Rh complex in the solution state was confirmed by UV–vis and Rh K-edge XAFS analysis.

After NaOH_{aq} was added to the aqueous Na₃RhCl₆ solution, the solution changed from dark red to clear yellow (Figure S1). In the UV–vis spectrum of the aqueous Na₃RhCl₆ solution, peaks at 509 and 403 nm corresponding to the *d–d* transition shifted to 422 and 335 nm,¹⁹ respectively, after NaOH_{aq} addition (Figure S2).²⁰ In the Rh K-edge XANES spectrum, the edge jump for the aqueous Na₃RhCl₆ solution appeared at higher energy than those of Rh foil and Rh₂O₃ reference standards (Figures 1a–c and Table S2), consistent with the

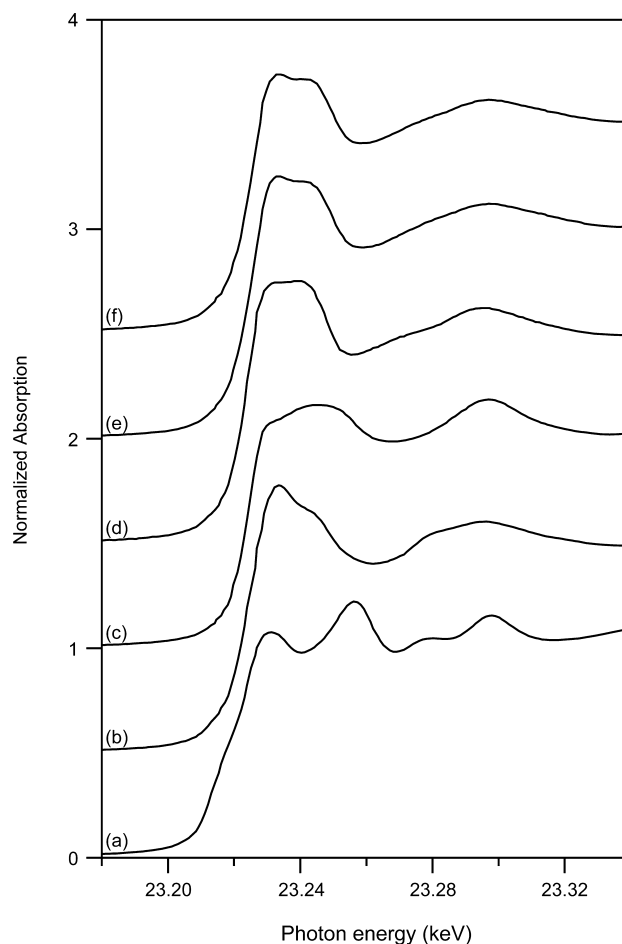


Figure 1. Rh K-edge XANES spectra for (a) Rh foil, (b) Rh₂O₃, (c) Na₃RhCl₆aq, (d) Na₃RhCl₆aq with NaOH, (e) fresh Rh/NiZn, and (f) the recovered Rh/NiZn catalyst.

presence of a high oxidation state (trivalent) Rh species. Subsequent NaOH_{aq} addition induced a significant change in the XANES line shape (Figure 1d) but had negligible impact upon the edge jump, indicating a change in the coordination environment but common oxidation state. Phase-shift uncorrected Fourier Transform (FT) of the *k*³-weighted Rh K-edge EXAFS spectra reveals the loss of a peak at ~0.19 nm, associated with a Rh–Cl bond, upon addition of NaOH_{aq} to Na₃RhCl₆, coincident with the appearance of a new scattering peak at ~0.15 nm associated with Rh–O bond formation; features characteristic of the Rh foil and Rh₂O₃ standards at 0.22, 0.25, and 0.32 nm (corresponding to Rh–Rh and Rh–O–Rh bonds) were absent (Figures 2a–d). Following phaseshift correction, the first peak in Figure 2d fitted well to a Rh–O scattering shell with six oxygen atoms at 0.206 nm for the Na₃RhCl₆ complex with NaOH_{aq} (Table 1). Hence UV–vis

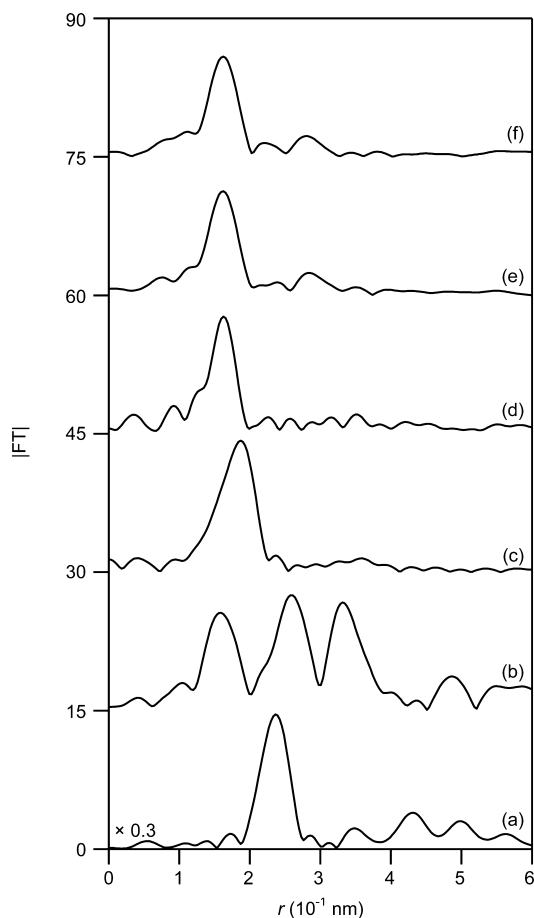


Figure 2. FT of k^3 -weighted Rh K-edge EXAFS spectra for (a) Rh foil, (b) Rh_2O_3 , (c) $\text{Na}_3\text{RhCl}_6\text{aq}$, (d) $\text{Na}_3\text{RhCl}_6\text{aq}$ with NaOH, (e) fresh Rh/NiZn, and (f) the recovered Rh/NiZn catalyst. Phase shifts were not corrected.

and Rh K-edge XAS evidenced the formation of an anionic $[\text{Rh}(\text{OH})_6]^{3-}$ complex in aqueous, basic solution.

Table 1. Curve-Fitting Results of Rh K-Edge EXAFS Spectra^a

sample	shell	CN ^b	r (nm) ^c	σ (nm) ^d
Rh foil ^e	Rh–Rh	(12)	(0.269)	
Rh_2O_3 ^e	Rh–O	(6)	(0.205)	
	Rh–(O)–Rh	(4)	(0.292)	
$\text{Na}_3\text{RhCl}_6\text{aq}$ ^e	Rh–Cl	(6)	(0.238)	
$\text{Na}_3\text{RhCl}_6\text{aq}$ + NaOH	Rh–O	6.0	0.206	0.0058
fresh Rh/NiZn	Rh–O	6.2	0.205	0.0057
recovered Rh/NiZn	Rh–O	5.9	0.205	0.0058

^aInverse FT were performed for the regions of 0.112–0.199 nm.

^bCoordination number. ^cBond distance. ^d σ is Debye–Waller factors.

^eData from X-ray crystallography.

Acetate anion-intercalated NiZn ($\text{CH}_3\text{COO}^-/\text{NiZn}$) was synthesized according to a previously reported procedure.¹⁶ The chemical formula and anion-exchange capacity of the parent NiZn were $\text{Ni}_{0.63}\text{Zn}_{0.37}(\text{OH})_2(\text{CH}_3\text{COO})_{0.37} \cdot 1.93\text{H}_2\text{O}$ (Ni/Zn = 2.20) and 2.44 mmol/g, respectively, on the basis of X-ray fluorescence (XRF) and thermogravimetric-differential thermal analysis (Figure S3 and Table S2). The rhodium species was intercalated into the NiZn interlayer via a simple

anion-exchange reaction in water. Treatment of $\text{CH}_3\text{COO}^-/\text{NiZn}$ with the aforementioned $[\text{Rh}(\text{OH})_6]^{3-}$ yielded the NiZn-intercalated Rh(III) hydroxyl complex, Rh/NiZn, as a green powder (Rh content: 0.034 mmol/g, as determined by AAS). XRD profiles revealed that the d_{001} peak shifted to a larger angle relative to the d_{001} peak of the parent $\text{CH}_3\text{COO}^-/\text{NiZn}$, with the associated C.S. (clearance space = basal spacing (d_{001}) – thickness of the brucite layer (0.46 nm)) falling to 0.36 nm for Rh/NiZn, from 0.84 nm for the parent NiZn (Figures 3a and

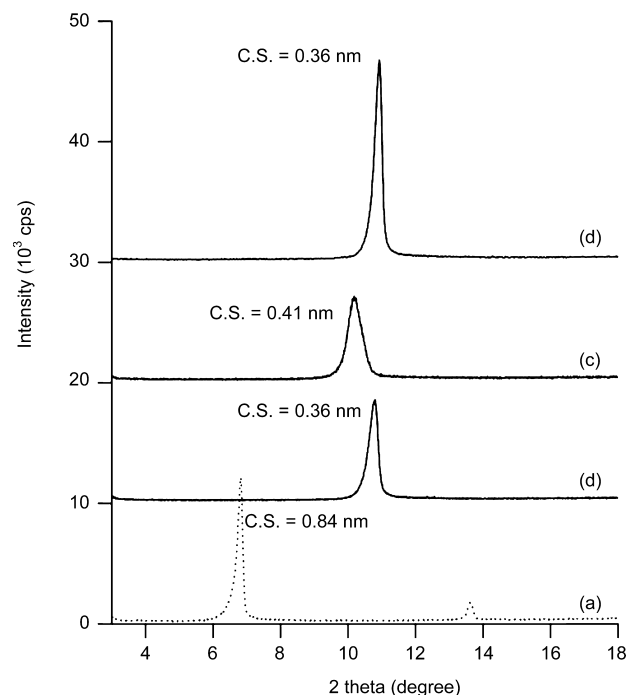


Figure 3. XRD profiles for (a) $\text{CH}_3\text{COO}^-/\text{NiZn}$, (b) Rh/NiZn, (c) recovered Rh/NiZn, and (d) OH^-/NiZn .

3b). The C.S. of OH^-/NiZn prepared by the same procedure but without the Rh species was also 0.36 nm (Figure 3d), suggesting that OH^- intercalation occurs alongside anionic Rh species under our strongly basic conditions. Additional experiments performed with a higher $[\text{Rh}(\text{OH})_6]^{3-}$ loading (0.5 mmol/g) evidenced a shift of the d_{001} peaks in the diffractogram to lower angle, indicative of an expanded interlayer clearance space (C.S.) as shown in Figure S6, confirming that $[\text{Rh}(\text{OH})_6]^{3-}$ must be incorporated within the NiZn interlayers.

X-ray photoelectron spectroscopy (XPS) was undertaken to determine the oxidation state of the Rh species within the NiZn interlayer. Figure 4 shows the Rh 3d XPS spectrum of Rh/NiZn, which fitted well to a unique chemical environment with a set of doublets (spin–orbit splitting = 4.74 eV) and $3d_{5/2}$ binding energy of 309.6 eV consistent with that of bulk Rh_2O_3 , i.e. a Rh(III) oxidation state,²¹ confirming a trivalent Rh species within the NiZn interlayer. The Ni 2p and Zn 2p XP spectra and Ni:Zn surface atomic ratios exhibited minimal changes following Rh exchange into the interlayer of the parent NiZn acetate (Figure S5), indicating the electronic structure and stoichiometry of the host cationic layers was preserved. Rh K-edge XAS (Figure 1e and 2e) of the Rh/NiZn solid were almost indistinguishable to those of the parent $[\text{Rh}(\text{OH})_6]^{3-}$ solution (Figure 1d and 2d); fitted EXAFS of the Rh/NiZn was likewise consistent with six oxygen atoms at 0.205 nm coordinated to a

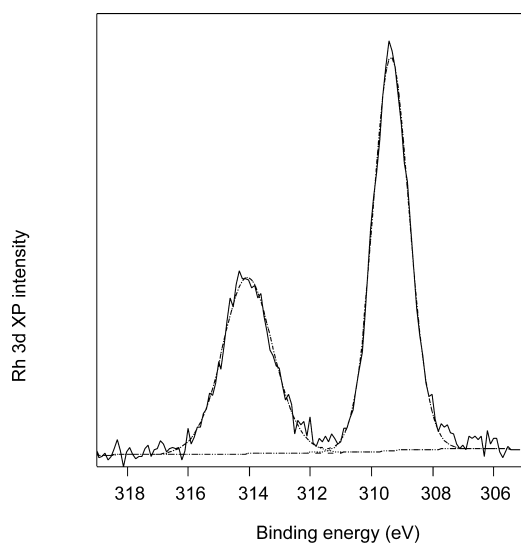
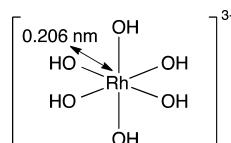


Figure 4. Fitted Rh 3d XP spectrum of the fresh Rh/NiZn catalyst.

monomeric Rh(III) center (Table 1). In concert, these observations demonstrate that the Rh species in the NiZn interlayer is a monomeric hexahydroxy rhodate anion, $[\text{Rh}(\text{OH})_6]^{3-}$, accompanied by intercalated OH^- , as shown in Scheme 1.

Scheme 1. Proposed Local Structure of Rh Species in a NiZn Interlayer



The efficiency of the resulting Rh/NiZn material toward 1,4-addition reactions was first explored employing a catalytic amount of 1,5-cyclooctadiene (1,5-COD). Previous homogeneous Rh complexes have shown the utility of 1,5-COD ligands for such 1,4-additions,¹⁰ in which their weak electron-donating effect upon Rh centers may accelerate transmetalation or addition of phenyl groups. 2-Cyclohexen-1-one (**1**) and phenylboronic acid (**2**) were chosen as model substrates for the initial optimization (Table 2), employing 0.034 g of the Rh/NiZn catalyst (1 μmol Rh), 1 mmol of substrate, and 0.5 equiv of 1,5-COD relative to Rh in a solvent mixture comprising 4 mL of toluene and 1 mL of water; stirred reactions were conducted at 100 °C under air. A 34% yield of 3-phenylcyclohexanone (**3**) was obtained after 1 h (entry 1). This was the only product observed in all reactions employing 2-cyclohexen-1-one. The amount of 1,5-COD was subsequently varied from 1 to 10 equiv relative to Rh (entries 1–7), with the best yield of 78% of **3** achieved using 6 equiv of 1,5-COD (entry 6). The impact of the toluene:H₂O solvent ratio was also explored (entries 7–10), with an equivolume mixture comprising 2.5 mL of toluene and 2.5 mL of H₂O affording a 92% yield (entry 10) after 1 h.²² TOFs approached 920 h⁻¹ per Rh under these reaction conditions, significantly higher than reported for alternative, heterogeneous Rh catalyst systems (polymer-intercalated chiral Rh/Ag bimetallic nanoparticles:¹³ 19 h⁻¹; recyclable polymer-Janaphos Rh:^{11a,b} 3.3 h⁻¹; Rh/HT:^{12a,b} 580 h⁻¹; RhFAP:^{12c} 17 h⁻¹; hydrophobized meso-

Table 2. Screening of Reaction Conditions for 1,4-Addition Reaction between **1** and **2** Catalyzed by Rh/NiZn^a

entry	toluene/H ₂ O (mL/mL)	1/2 (mmol/mmol)	1,5-COD (equiv relative to Rh)	yield (%) ^b
1	4/1	1/1	0.5	34
2	4/1	1/1	1	47
3	4/1	1/1	2	54
4	4/1	1/1	3	64
5	4/1	1/1	5	73
6	4/1	1/1	6	78
7	4/1	1/1	10	69
8	4.5/0.5	1/1	6	39
9	3.3/1.7	1/1	6	81
10	2.5/2.5	1/1	6	92
11	2.5/2.5	1/2	6	64
12	2.5/2.5	1/3	6	34
13 ^c	2.5/2.5	1/1	6	nd
14 ^d	2.5/2.5	1/1	6	nd
15 ^e	2.5/2.5	1/1	6	nd

^aRh/NiZn catalyst (Rh: 1 μmol), **1** (1 mmol), **2**, 1,5-COD, solvent (5 mL), 100 °C, air 1 h. ^bDetermined by GC using an internal standard technique. ^cWithout catalyst. ^dCH₃COO⁻/NiZn (0.05 g). ^eOH⁻/NiZn (0.05 g).

porous silica-grafted Rh:^{12c,d} 12 h⁻¹; Rh-TPPTS/HT:^{12f} 5.3 h⁻¹; PS-PEG-supported Rh:^{11d} 1.4 h⁻¹; and chiral PS-supported Rh:^{11c} 3.3 h⁻¹). The order in phenylboronic acid **2** was also investigated (entries 10–12), revealing an inverse dependence on 3-phenylcyclohexanone yield; maximal yield of **3** was obtained for one equivalent of **2**, indicating that excess phenylboronic acid may inhibit the catalytic cycle. This latter phenomenon was not observed in studies employing a polymer-Janaphos Rh catalyst and 1.3 equiv of **2**.^{11a,b} Control reactions showed negligible activity in the absence of catalyst or using the parent CH₃COO⁻/NiZn or OH⁻/NiZn without incorporated Rh species (entries 13–15). Catalytic activity was strongly dependent on the choice of olefin (Table 3), with 1,5-COD unique as the only diene to significantly promote the addition reaction (entry 1);²³ 1,3-cyclooctadiene, 1,4-cyclo-

Table 3. Effect of Olefins on the Rh/NiZn-Catalyzed 1,4-Addition Reaction^a

entry	olefin	yield of 3 (%) ^b
1	1,5-cyclooctadiene	92
2	1,3-cyclooctadiene	5
3	1,4-cyclohexadiene	trace
4	2,5-norbornadiene	4
5	1,5-hexadiene	15
6	cyclooctene	trace
7	cyclohexene	trace
8	2-norbornene	trace
9	1,5,9-cyclododecatriene	4
10	none	nd

^aRh/NiZn catalyst (Rh: 1 μmol), **1** (1 mmol), **2** (1 mmol), olefin (6 equiv relative to Rh), toluene (2.5 mL), H₂O (2.5 mL), 100 °C, air, 1 h. ^bDetermined by GC using an internal Standard technique.

hexadiene, 2,5-norbornadiene, 1,5-hexadiene, and 1,5,9-cyclododecatriene proved ineffective (entries 2–5 and 9). No reaction occurred in the presence of monoenes such as cyclooctene, cyclohexene, and 2-norbornene (entries 6–8) or in the absence of olefins (entry 9). This suggests that the 1,5-COD ligand may coordinate to Rh during reaction to form a stable, activated complex.

The 1,4-addition between **1** and **2** catalyzed by Rh/NiZn was also successfully undertaken on a preparative scale. For example, **1** (0.96 g; 10 mmol) and **3** (1.21 g; 10 mmol) successfully gave **3** (1.62 g; 93% of isolated yield) in the presence of the Rh/NiZn catalyst (0.1 g, Rh: 0.029 mol %) for 4 h, wherein the TON was up to 3200.

The superior activity and selectivity of Rh/NiZn for 1,4-addition reactions was apparent from benchmarking against a range of alternative rhodium catalysts such as Rh⁰/carbon, Rh₂O₃, and Rh(OH)₃ under the same reaction conditions (Table 4). RhCl₃·*n*H₂O and Na₃RhCl₆·12H₂O also afforded **3**

Table 4. 1,4-Addition Reaction between **1** and **2** with Various Rh Catalysts^a

entry	Rh catalyst	yield of 3 (%) ^b
1	Rh/NiZn	92
2 ^c	Rh ⁰ /carbon (5 wt %)	trace
3	Rh ₂ O ₃	trace
4	Rh(OH) ₃	trace
5	RhCl ₃ · <i>n</i> H ₂ O	80
6	Na ₃ RhCl ₆ ·12H ₂ O	61

^aRh catalyst (Rh: 1 μmol), **1** (1 mmol), **2** (1 mmol), 1,5-COD (6 equiv relative to Rh), toluene (2.5 mL), H₂O (2.5 mL), 100 °C, air, 1 h. ^bDetermined by GC using an internal standard technique. ^cPurchased from Aldrich.

in moderate yields of 80% and 61%, respectively (entries 5 and 6). Anionic [Rh(OH)₆]³⁻ intercalated into the NiZn interlayer thus appears a highly efficient catalyst for this coupling reaction, attributed to a strong electrostatic interaction between NiZn sheets and interlayer [Rh(OH)₆]³⁻ species which hinders their deactivation via Rh aggregation into Rh₂O₃ or metal nanoparticles, as common with other unstabilized complexes.^{12b,24}

In order to assess whether the Rh/NiZn catalyst underwent on-stream deactivation by e.g. restructuring of the active metal species or HDS layers, or leaching of Rh into the reaction mixture, an experiment was conducted in which additional quantities of reactants **1** and **2** were added to the reaction mixture following an initial catalytic run. Figure 5 shows that 1,4-addition of the second batch of reactants proceeded identically over the used catalyst, with no change in kinetics of **3** production, while elemental analysis (AAS) of the filtrate evidenced negligible leached Rh (below 4 × 10⁻⁶ g).²⁵ Spectroscopic analysis confirmed the stability of our Rh/NiZn catalyst, with Rh K-edge XANES and fitted EXAFS of fresh and spent materials indistinguishable (Figures 1d, 2d and Table 1). These measurements confirm that Rh species within the NiZn matrix remain in a trivalent, monomeric state throughout the 1,4-addition reaction; a strong electrostatic interaction between anionic [Rh(OH)₆]³⁻ species and the layered NiZn host is hypothesized to inhibit rhodium aggregation. The C.S. of the recovered Rh/NiZn catalyst expanded slightly from 0.36 to 0.41 nm (Figure 3b and 3c), which may reflect interlayer water incorporation alongside [Rh(OH)₆]³⁻ and OH⁻ anions during reaction. It seems highly

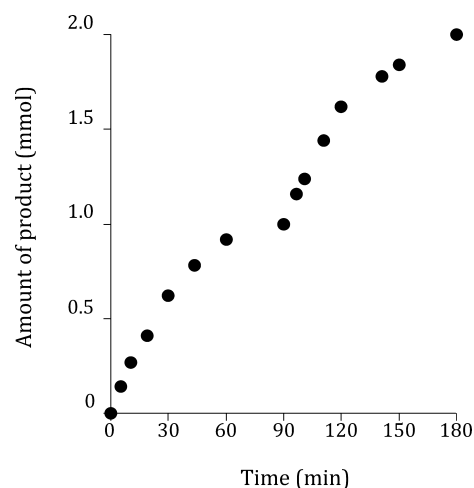


Figure 5. Time profile of 1,4-addition reaction of **1** and **2** in the presence of the Rh/NiZn catalyst. Reaction conditions: Rh/NiZn catalyst (Rh: 0.12 mol %) **1** (1 mmol), **2** (1 mmol), 1,5-COD (1 equiv relative to Rh), toluene/H₂O (5 mL, v/v: 5/1), 100 °C.

probable that catalysis is confined within the NiZn interlayers; Rh leaching was not observed by AAS or any changes in environment by XAS (Figures 1f and 2f), and the parent CH₃COO⁻/NiZn or OH⁻/NiZn were unable to catalyze reaction in its absence (Table 2, entries 14 and 15), it is inconceivable that migration out from the interlayers would not result in solution phase Rh detectable by elemental analysis or significant changes in the Rh chemical environment.

The scope of 1,4-addition reactions was examined for a variety of electron-deficient olefin substrates (Table 5) under

Table 5. Substrate Screening of 1,4-Addition Reaction with the Rh/NiZn Catalyst^a

Entry	Enone	Boronic acid	Time (h)	Product	Yield (%) ^b
1 ^c		2	2		84
2		2	2		92
3	1		1		92
4		R = H	2	R = H	95
5		CH ₃	2	CH ₃	84
6		OCH ₃	2	OCH ₃	98
		Cl	2	Cl	98
7 ^d		2	12		87
8 ^d		2	6		>99

^aRh/NiZn catalyst (0.034 g, Rh: 0.1 mol %), enone (1 mmol), boronic acid (1 mmol), 1,5-COD (6 equiv relative to Rh), toluene/H₂O (5 mL, 1/1 v/v), 100 °C. ^bDetermined by GC using an internal standard technique. ^cEnone (2 mmol). Yield was based on **2**. ^dRh/NiZn (0.068 g, Rh: 0.2 mol %)

optimized conditions using a 1,5-COD and 1:1 toluene:H₂O mixed solvent. 3-Buten-2-one and 2-cyclopentan-1-one were good acceptors for the reaction with **2** (entries 1 and 2). 3-Nonen-2-one and chalcone also reacted with **2**, generating 4-phenyl-nonan-2-one and 1,3,3-triphenylpropan-1-one, respectively, in excellent yields (entries 7 and 8). Rh/NiZn was also efficacious toward various *p*-substituted phenylboronic acids (entries 3–6), resulting in high yields of coupled products. We propose the following reaction pathway for 1,4-additions catalyzed by Rh/NiZn, which mirrors that previously reported for homogeneous Rh catalysts: (i) transmetalation of the interlayer [Rh(OH)₆]³⁻ species and arylboronic acid to generate a Rh–Ar species; (ii) olefin insertion into the Rh–Ar bond, yielding an oxa- π -allyl rhodium enolate, which is readily protonated by water; (iii) elimination of the desired addition product, regenerating the initial [Rh(OH)₆]³⁻ species. Phenylboronic acids might also be quarternized with interlayer OH⁻ anions to facilitate transmetalation to [Rh(OH)₆]³⁻.²⁶

4. CONCLUSIONS

Synthesis of a well-defined [Rh(OH)₆]³⁻/NiZn catalyst system which efficiently catalyzes the 1,4-addition reaction between various enones and phenylboronic acids into their corresponding β -substituted carbonyl compounds has been demonstrated. The intercalated, monomeric, trivalent Rh hydroxide species was stabilized by the NiZn matrix during reaction, enabling recycling with negligible deactivation. We are currently investigating the application of our catalyst toward asymmetric 1,4-addition reactions and the hydrophenylation of internal alkynes with phenylboronic acid into substituted alkenes for which we have obtained promising preliminary results.

■ ASSOCIATED CONTENT

Supporting Information

The photoimages of preparation solution, UV–vis spectra, TG-DTA data, bulk Ni/Zn ratio and surface elemental composition, the E_0 values in Rh *K*-edge XANES, curve-fitting results of FT of EXAFS, XPS, and NMR data. This material is available free of charge via the Internet at <http://pubs.acs.org>.

■ AUTHOR INFORMATION

Corresponding Author

*E-mail: shimazu@faculty.chiba-u.jp.

Notes

The authors declare no competing financial interest.

■ ACKNOWLEDGMENTS

This study was supported by a Grant-in-Aid for Scientific Research from the Ministry of Education, Culture, Sports, Science, and Technology of Japan (25420824). The Rh *K*-edge XAFS experiments were conducted at a facility in the Photon Factory (KEK-PF, Proposal No. 2012G596). We are also grateful to Mr. Muneharu Nozawa and Ms. Tomoko Fukusaki for their invaluable contributions to the work described here. A.F.L. thanks the EPSRC for the award of a Leadership Fellowship (EP/G007594/4), and K.W. thanks the Royal Society for the award of an Industry Fellowship.

■ REFERENCES

(1) For book, reviews, and accounts, see: (a) Omwoma, S.; Chen, W.; Tsunashima, R.; Song, Y.-F. *Coord. Chem. Rev.* **2014**, *258*, 258–259, 58–71. (b) He, S.; An, Z.; Wei, M.; Evans, D. G.; Duan, X. *Chem.*

Commun. **2013**, *49*, 5912–5920. (c) Wang, Q.; O'Hare, D. *Chem. Rev.* **2012**, *112*, 4124–4155. (d) Oliver, S. R. *J. Chem. Soc. Rev.* **2009**, *38*, 1868–1881. (e) Kaneda, K.; Ebitani, K.; Mizugaki, T.; Mori, K. *Bull. Chem. Soc. Jpn.* **2006**, *79*, 981–1016. (f) de Roy, A.; Forano, C.; El Malki, K.; Basse, J.-P. In *Expanded Clays and Other Microporous Solids*; Occelli, M. L.; Robson, H. E., Eds.; Van Nostrand Reinhold: New York, 1992; pp 108–169.

(2) (a) Bull, R. M. R.; Markland, C.; Williams, G. R.; O'Hare, D. *J. Mater. Chem.* **2011**, *21*, 1822–1828. (b) Rajamathi, J. T.; Arulraj, A.; Ravishankar, N.; Arulraj, J.; Rajamathi, M. *Langmuir* **2008**, *24*, 11164–11168. (c) Arizaga, G. G. C.; Satyanarayana, K. G.; Wypych, F. *Solid State Ionics* **2007**, *178*, 1143–1162. (d) Yang, J.-H.; Han, Y.-S.; Park, M.; Park, T.; Hwang, S.-J.; Choy, Y.-S. *Chem. Mater.* **2007**, *19*, 2679–2685. (e) Morioka, H.; Tagaya, H.; Karasu, M.; Kadokawa, J.; Chiba, K. *Inorg. Chem.* **1999**, *38*, 4211–4216. (f) Yamanaka, S.; Sako, T.; Seki, K.; Hattori, M. *Solid State Ionics* **1992**, *53–56*, 527–533.

(3) (a) Hara, T.; Sawada, J.; Nakamura, Y.; Ichikuni, N.; Shimazu, S. *Catal. Sci. Technol.* **2011**, *1*, 1376–1382. (b) Hara, T.; Kurihara, J.; Ichikuni, N.; Shimazu, S. *Chem. Lett.* **2010**, *39*, 304–305. (c) Hara, T.; Ishikawa, M.; Sawada, J.; Ichikuni, N.; Shimazu, S. *Green Chem.* **2009**, *11*, 2034–2040.

(4) (a) Sathisha, T. V.; Swamy, B. E. K.; Chandrashekar, B. N.; Thomas, N.; Eswarappa, B. *J. Electroanal. Chem.* **2012**, *674*, 57–64. (b) Delorme, F.; Seron, A.; Licheron, M.; Veron, E.; Giovannelli, F.; Beny, C.; Jean-Prost, V.; Martineau, D. *J. Solid State Chem.* **2009**, *182*, 2350–2356. (c) Kandare, E.; Hossenlopp, J. M. *Inorg. Chem.* **2006**, *45*, 3766–3773. (d) Rojas, R.; Barriga, C.; Ulibarri, M. A.; Malet, P.; Rives, V. *J. Mater. Chem.* **2002**, *12*, 1071–1078. (e) Choy, J.-H.; Kwon, Y.-M.; Han, K.-S.; Song, W.-W.; Chang, S.-H. *Mater. Lett.* **1998**, *34*, 356–363. (e) Nishizawa, H.; Yuasa, K. *J. Solid State Chem.* **1998**, *141*, 229–234. (f) Choy, J.-H.; Kwon, Y.-M.; Song, W.-W.; Chang, S.-H. *Bull. Korean Chem. Soc.* **1997**, *18*, 450–453. (g) Komaeneni, S.; Li, Q. H.; Roy, R. *J. Mater. Res.* **1996**, *11*, 1866–1869. (h) Meyn, M.; Beneke, K.; Lagaly, C. *Inorg. Chem.* **1993**, *32*, 1209–1215.

(5) (a) Rajamathi, J. T.; Raviraj, N. H.; Ahmed, M. F.; Rajamathi, M. *Solid State Sci.* **2009**, *11*, 2080–2085. (b) Rojas, R.; Ulibarri, M. A.; Barriga, C.; Rives, V. *Microporous Mesoporous Mater.* **2008**, *112*, 262–272. (c) Rojas, R.; Barriga, C.; Ulibarri, M. A.; Rives, V. *J. Solid State Chem.* **2004**, *177*, 3392–3401.

(6) (a) Kandare, E.; Hossenlopp, J. M. *J. Phys. Chem. B* **2005**, *109*, 8469–8475. (b) Tronto, J.; Leroux, F.; Dubois, M.; Taviot-Gueho, C.; Valim, J. *J. Phys. Chem. Solids* **2006**, *67*, 978–982. (c) Arulraj, J.; Rajamathi, J. T.; Prabhu, K. R.; Rajamathi, M. *Solid State Sci.* **2007**, *9*, 812–816. (d) Richardson-Chong, S. S. D.; Patel, R.; Williams, G. R. *Ind. Eng. Chem. Res.* **2012**, *51*, 2913–2921.

(7) (a) Nityashree, N.; Rajamathi, M. *J. Phys. Chem. Solids* **2013**, *74*, 1164–1168. (b) Rajamathi, J. T.; Ravishankar, N.; Rajamathi, M. *Solid State Sci.* **2005**, *7*, 195–199.

(8) For reviews, see: (a) Tian, P.; Dong, H.-Q.; Lin, G.-Q. *ACS Catal.* **2012**, *2*, 95–119. (b) Edwards, H. J.; Hargrave, J. D.; Penrose, S. D.; Frost, C. G. *Chem. Soc. Rev.* **2010**, *39*, 2093–2105. (c) Defieber, C.; Grützmacher, H.; Carreira, E. M. *Angew. Chem., Int. Ed.* **2008**, *47*, 4482–4502. (d) Miyaura, N. *Bull. Chem. Soc. Jpn.* **2008**, *81*, 1535–1553. (e) Hayashi, T.; Yamasaki, K. *Chem. Rev.* **2003**, *103*, 2829–2844.

(9) Sakai, M.; Hayashi, H.; Miyaura, N. *Organometallics* **1997**, *16*, 4229–4231.

(10) Recently reported examples, see: (a) Korenaga, T.; Ko, A.; Shimada, K. *J. Org. Chem.* **2013**, *78*, 9975–9980. (b) Khair, N.; Salvador, Á.; Valdivia, V.; Chelouan, A.; Alcudia, A.; Álvarez, E.; Fernández, I. *J. Org. Chem.* **2013**, *78*, 6510–6521. (c) Takaya, H.; Iwaya, T.; Ogata, K.; Isozaki, K.; Yokoi, T.; Yoshida, R.; Yasuda, N.; Seike, H.; Takenaka, T.; Nakamura, M. *Synlett* **2013**, *24*, 1910–1914. (d) Chen, Q.; Chen, C.; Guo, F.; Xia, W. *Chem. Commun.* **2013**, *49*, 6433–6435. (e) Fairhurst, N. W. G.; Munday, R. H.; Carbery, D. R. *Synlett* **2013**, *24*, 496–498.

(11) (a) Jana, R.; Tunge, J. A. *J. Org. Chem.* **2011**, *76*, 8376–8385. (b) Jana, R.; Tunge, J. A. *Org. Lett.* **2009**, *11*, 971–974. (c) Otomatsu, Y.; Senda, T.; Hayashi, T. *Org. Lett.* **2004**, *6*, 3357–3359. (d) Uozumi, Y.; Nakazono, M. *Adv. Synth. Catal.* **2002**, *344*, 274–277.

- (12) (a) Motokura, K.; Hashimoto, N.; Hara, T.; Mitsudome, T.; Mizugaki, T.; Jitsukawa, K.; Kaneda, K. *Green Chem.* **2011**, *13*, 2416–2422. (b) Fujita, N.; Motokura, K.; Mori, K.; Mizugaki, T.; Ebitani, K.; Jitsukawa, K.; Kaneda, K. *Tetrahedron Lett.* **2006**, *47*, 5083–5087. (c) Handa, P.; Holmberg, K.; Sauthier, M.; Castanet, Y.; Mortreux, A. *Microporous Mesoporous Mater.* **2008**, *116*, 424–431. (d) Handa, P.; Witula, T.; Reis, P.; Holmberg, K. *ARKIVOC* **2008**, 107–118. (e) Kantam, M. L.; Subrahmanyam, V. B.; Kumar, K. B. S.; Venkanna, G. T.; Sreedhar, B. *Helv. Chim. Acta* **2008**, *91*, 1947–1953. (f) Neatu, F.; Besnea, M.; Komvokis, V. G.; Genêt, J.-P.; Michelet, V.; Triantafyllidis, K. S.; Pârvulescu, V. I. *Catal. Today* **2008**, *139*, 161–167.
- (13) Yasukawa, T.; Miyamura, H.; Kobayashi, S. *J. Am. Chem. Soc.* **2012**, *134*, 16963–16966.
- (14) Itaoka, R.; Iguchi, Y.; Miyaura, N. *Chem. Lett.* **2001**, *30*, 722–723.
- (15) Hayashi, T.; Takahashi, M.; Takaya, Y.; Ogasawara, M. *J. Am. Chem. Soc.* **2002**, *124*, 5052–5058.
- (16) Yamanaka, S.; Ando, K.; Ohashi, M. *Mater. Res. Symp. Proc.* **1995**, *371*, 131–142.
- (17) (a) Baes, C. F., Jr.; Mesmer, R. E. *The Hydrolysis of Cations*; Krieger Publishing Company: FL, 1976. (b) Ivanon-Emin, B. N.; Borzova, L. D.; Egorov, A. M.; Malyugina, S. G. *Russ. J. Inorg. Chem.* **1971**, *16*, 1474–1476. (c) Dolzhenko, V. D.; Komozin, P. N.; Evtushenko, E. G.; Kiselev, Y. M. *Russ. J. Inorg. Chem.* **2002**, *47*, 692–698.
- (18) Lederer, M.; Leipzig-Pagani, E.; Lumini, T.; Roulet, R. *J. Chromatogr. A* **1997**, *769*, 325–332.
- (19) (a) Dai, Z.-M.; Burgeth, G.; Parrino, F.; Kisch, H. *J. Organomet. Chem.* **2009**, *694*, 1049–1054. (b) Schmidtke, H.-H. *Z. Phys. Chem. Neue Folge* **1965**, *45*, 305–316.
- (20) Photographic images of the preparation solution are displayed in Figure S1, Supporting Information; the UV–vis spectra and presented in Figure S2.
- (21) Lee, A. F.; Seabourne, C. R.; Wilson, K. *Catal. Commun.* **2006**, *7*, 566–570.
- (22) Catalytic reaction also proceeded effectively without stirring as seen in Table 2, entry 10.
- (23) In the FT-IR spectrum of this Rh/NiZn catalyst with 1,5-COD, no significant change of the spectrum was observed, due to the low loading amount of the guest $[\text{Rh}(\text{OH})_6]^{3-}$ complex. The weak electron-donating effect of 1,5-COD ligand on a Rh center may accelerate the reaction rate.
- (24) (a) King, R. B.; Bhattacharyya, N. K. *Inorg. Chim. Acta* **1995**, *237*, 65–69. (b) Fujitsu, H.; Matsunuma, E.; Takeshita, K.; Mochida, I. *J. Org. Chem.* **1981**, *46*, 5353–5357.
- (25) In contrast, recovery of the Rh/NiZn catalyst via filtration/centrifugation, washing, and drying, lowered its activity upon subsequent reuse, resulting in yields of **3** below 40% as summarized in Tables S3 and S4 of the Supporting Information.
- (26) Itooka, R.; Iguchi, Y.; Miyaura, N. *J. Org. Chem.* **2003**, *68*, 6000–6004.